Article

Self-Assembling Peptide as a Potential Carrier of Hydrophobic Compounds

Christine Keyes-Baig, Jean Duhamel, Shan-Yu Fung, Jeremy Bezaire, and P. Chen

J. Am. Chem. Soc., **2004**, 126 (24), 7522-7532• DOI: 10.1021/ja0381297 • Publication Date (Web): 28 May 2004

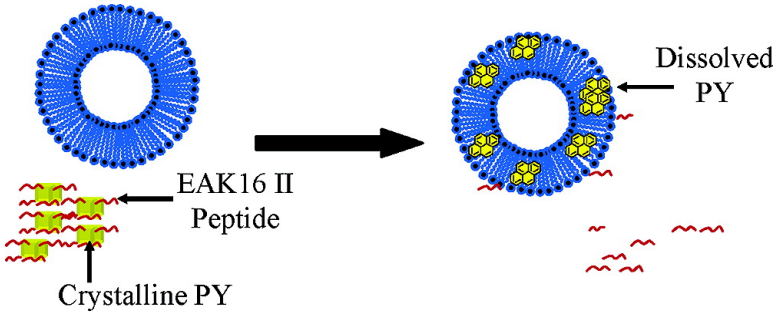

More About This Article

Additional resources and features associated with this article are available within the HTML version:

- Supporting Information
- Links to the 4 articles that cite this article, as of the time of this article download
- Access to high resolution figures
- Links to articles and content related to this article
- Copyright permission to reproduce figures and/or text from this article

View the Full Text HTML

J|A|C|S
ARTICLES
Published on Web 05/28/2004

Self-Assembling Peptide as a Potential Carrier of Hydrophobic Compounds

Christine Keyes-Baig,[†] Jean Duhamel,*[,†] Shan-Yu Fung,[‡] Jeremy Bezaire,[‡] and P. Chen[‡]

Contribution from the Department of Chemistry and Department of Chemical Engineering, Contribution from the University of Waterloo, 200 University Avenue West, Waterloo, Ontario N2L 3G1, Canada

Received August 26, 2003; E-mail: jduhamel@uwaterloo.ca

Abstract: Microcrystals of a hydrophobic cargo were stabilized by EAK16 II, a self-assembling oligopeptide, and suspended in aqueous solution. Pyrene was used as a model hydrophobic compound. Egg phosphatidylcholine (EPC) vesicles were prepared to mimic a cell membrane. Pyrene was released from its EAK16 II coating into EPC vesicles. The excimer decay profiles were acquired. They showed that pyrene is present in the crystalline form when stabilized by EAK16 II, it is molecularly dispersed in EPC vesicles, and it is completely released from its EAK16 II coating into the membrane bilayers. The release of pyrene from the microcrystals coated with EAK16 II into the EPC membrane was followed by fluorescence as a function of time. The amount of pyrene released into the EPC vesicles at a given time was quantified using a calibration curve. The concentration of pyrene released was determined as a function of time, and the concentration-versus-time profile was fitted with one exponential. The rate of pyrene release was found to depend on the peptide-to-pyrene molecular ratio. Higher peptide-to-pyrene ratios lead to slower transfer of pyrene to the lipophilic environment. Scanning electron micrographs demonstrated that a thicker coating on the pyrene crystals results in a slower release. The data presented in this work demonstrate that the self-assembling EAK16 II can stabilize a hydrophobic cargo in aqueous solution and deliver it into a lipophilic environment, and that the rate of transfer can be adjusted by tuning the peptide-to-pyrene ratio.

Introduction

The serendipitous discovery 10 years ago that peptides bearing repeating sequences of both ionic and hydrophobic amino acids are capable of self-assembling spontaneously into various microstructures in aqueous solution[1] triggered numerous studies aiming at synthesizing novel self-assembling peptides (referred to as sapeptides) and characterizing the resulting microstructure.[2] The potential applications for the biomaterials generated by these novel self-assembling peptides range from scaffolding for tissue repair in regenerative medicine, drug delivery, and biological surface engineering. While proofs of principle have been provided for the use of sapeptides in scaffolding[3] and biological surface engineering,[4] no study has yet been carried out to investigate the applicability of sapeptides as drug carriers. We report herein how the EAK16 II sapeptide is capable of stabilizing microcrystals of a hydrophobic compound and delivering it into the membrane of a cell mimic.

EAK16 II is a peptide made of 16 amino acids with alternating pairs of positive and negative charges separated by a hydrophobic amino acid residue (Ala).[1] At neutral pH, Glu and Lys are negatively and positively charged, respectively. They are believed to form complementary ion pairs when EAK16 II self-assembles into its β-sheet microstructure which exhibits a hydrophobic and a hydrophilic surface.[1−3] These β-sheets form fibrils exhibiting a diameter of 50 ± 20 nm and length of up to 1 μm and further assemble into macroscopic membranes which have shown good stability under harsh treatments such as acidic/basic conditions (pH 1.5, 3.0, 7.0, 11) or media containing various proteases (trypsin, α-chymotrypsin, papin protease K, and Pronase).[1,5] These combined features make EAK16 II an ideal candidate as a carrier of hydrophobic cargoes. As a carrier, the hydrophobic surface of the β-sheet would interact with the hydrophobic cargo, whereas its hydrophilic surface would ensure solubility in aqueous solution. From this point on, the term EAK will refer to the EAK16 II sapeptide.

Numerous drugs are insoluble in water and require an appropriate vehicle to deliver them to a given target cell or tissue.[6] Block copolymer micelles[7−12] and vesicles,[13] lipo-

[†] Department of Chemistry.
[‡] Department of Chemical Engineering.

(1) Zhang, S.; Holmes, T.; Lockshin, C.; Rich, A. *Proc. Natl. Acad. Sci. U.S.A.* **1993**, *90*, 3334−3338.
(2) Zhang, S. *Biotechnol. Adv.* **2002**, *20*, 321−339. Zhang, S.; Altman, M. *React. Funct. Polym.* **1999**, *41*, 91−102. Zhang, S.; Marini, D. M.; Hwang, W.; Santoso, S. *Curr. Opin. Chem. Biol.* **2002**, *6*, 865−871.
(3) Zhang, S.; Holmes, T. C.; DiPersio, C. M.; O. Hynes, R.; Su, X.; Rich, A. *Biometerials* **1995**, *16*, 1385−1393. Holmes, T. C.; de Lacalle, S.; Su, X.; Liu, G.; Rich, A.; Zhang, S. *Proc. Natl. Acad. Sci. U.S.A.* **2000**, *97*, 6728−6733.
(4) Zhang, S.; Yan, L.; Altman, M.; Lässle, M.; Nugent, H.; Frankel, F.; Lauffenburger, D. A.; Whitesides, G. M.; Rich, A. *Biomaterials* **1999**, *20*, 1213−1220.
(5) Fung, S. Y.; Keyes, C.; Duhamel, J.; Chen, P. *Biophys. J.* **2003**, *85*, 537−548.
(6) Gershanik, T.; Benita, S. *Eur. J. Pharm. Biopharm.* **2000**, *50*, 179−188.

10.1021/ja0381297 CCC: $27.50

somes,[8b,14] and gel micro-encapsulations[15−18] are examples of delivery systems for hydrophobic drugs. Each one of these systems has been designed to provide hydrophobic microdomains in aqueous solution, which can accommodate a hydrophobic cargo. For instance, block copolymers made of a hydrophilic chain connected to a hydrophobic one, self-assemble into micelles or vesicles where the hydrophobic micelle core or vesicle membrane is stabilized by the hydrophilic corona.[7−13] Liposomes exhibit a lipid bilayer whose interior is lined by the hydrophobic lipid tails.[8b,14] Oil microemulsions can be entrapped inside a gel to provide water-stable microspheres encapsulating oily droplets.[15,16] Compared to these well-characterized delivery systems, much less is known about the ability of oligopeptides at carrying and delivering a hydrophobic compound in aqueous solution.

This work reports the spontaneous formation of colloids of pyrene crystals stabilized by EAK adsorbed onto their surface. Pyrene was chosen as a model of a hydrophobic cargo.[7b−c,9−11,41a−b,43] Its well characterized fluorescence was used to assign whether it was present in the peptide matrix as individual molecules or microcrystals.[19] It also allowed the determination of the rate at which pyrene migrates from the colloidal crystals stabilized by EAK into membrane bilayers made of the egg phosphatidylcholine (EPC) liposomes. The ability of the self-assembling EAK carrier to unload its hydrophobic cargo into a lipophilic domain demonstrates its potential as a carrier of hydrophobic compounds and opens venues for the design of new self-assembling peptides to be used as delivery systems. The use of a peptide as an efficient colloidal stabilizer for a hydrophobic compound represents a departure from the more common drug delivery applications associated with carrier peptides, which typically enhance cell adhesion[20] or cell barrier translocation.[21] In such applications, the peptidic or chemical drug is covalently attached to the carrier peptide to form a chimeric peptide.

Experimental Section

Chemicals. EAK was purchased from Research Genetics. Egg Phosphatidylcholine (EPC) in chloroform (20 mg/mL) was obtained from Avanti Polar Lipids, Inc. Pyrene was obtained from Sigma Aldrich. Pyrene was subsequently recrystallized three times from ethanol. Ethylenediaminetetraacetic acid (EDTA) was purchased from Bio-Rad Laboratories and used as received. Tris (hydroxymethyl) methylamine (Tris) and acetic acid were obtained from BDH Inc. Double distilled water (deionized from Millipore Milli-RO 10 Plus and Milli-Q UF Plus, Bedford, MA) was used in all solution preparations.

Vesicle Preparation. EPC in chloroform (75 g) was added to a 1 L round-bottom flask. The chloroform was then evaporated off using a rotary evaporator to produce a thin film inside the round-bottom flask. The film was dispersed at room temperature in 310 mL of a buffer solution containing 25 mM Tris/acetic acid (pH = 7.0) and 0.2 mM EDTA.[22] The mixture was then sonicated for 25−30 min in a sonifier cell disrupter (Heat Systems-Ultrasonic Inc, model W-225) set at about 20 W output.[23] The round-bottom flask was kept near 0 °C on ice above the lipid phase transition temperature (T_c= −15 °C to −7 °C[22,24]) and nitrogen was bubbled into the mixture. This was followed by centrifugation at 7000 rpms for 1 h to eliminate the larger membranes and eventual titanium particles from the sonifier probe.[23] The supernatant was collected and stored at 5 °C. Two lipid concentrations were used, either 6.9×10^{-4} or 7.4×10^{-4} M.

Determination of the Lipid Concentration. Three known masses of the vesicle solution were pipetted into preweighed 20 mL vials. Three aliquots of the Tris/acetic acid and EDTA buffer solution with masses close to the mass of the vesicle solution were also pipetted into preweighed 20 mL vials. This was done so that the solid content of the buffer solution could be withdrawn from the mass of the dried liposome and an accurate concentration of the EPC lipid could be determined. The three sets of vesicle and buffer solutions were set under a stream of nitrogen to obtain a film at the bottom of the vial. The vials were then placed in a vacuum oven overnight at 60 °C to remove any traces of water. The mass of the three sets of vesicle and buffer films were obtained and the average concentration of the vesicle solution and the buffer solution was calculated in g/mL. The deviation from the average concentration was always smaller than 2.50%. The concentration of the EPC solution was determined by taking the difference between the solid content of the vesicle solution and that of the buffer solution.

Preparation of Stable Suspensions of Pyrene Crystals. Two solutions of EAK and pyrene (PY) crystals were prepared by placing weighed amounts of the peptide and pyrene in a 20 mL vial and dissolving in water to obtain concentrations of 5.0 ×

(7) (a) Yokoyama, M.; Kwon, G. S.; Okano, T.; Sakurai, Y.; Seto, T.; Kataoka, K. *Bioconjugate Chem.* **1992**, *3*, 295−301. (b) Kwon, G. S.; Naito, M.; Kataoka, K.; Yokoyama, M.; Sakurai, Y.; Okano, T. *Colloids Surf. B: Biointerfaces* **1994**, *2*, 429−434. (c) Liaw, J.; Aoyagi, T.; Kataoka, K.; Sakurai, Y.; Okano, T. *Pharmaceutical Res.* **1998**, *15*, 1721−1726. (d) Kataoka, K.; Kwon, G. S.; Yokoyama, M.; Okano, T.; Sakurai, Y. *J. Control. Release* **1993**, *24*, 119−132. (e) Kwon, G.; Suwa, S.; Yokoyama, M.; Okano, T.; Sakurai, Y.; Kataoka, K. *J. Control. Release* **1994**, *29*, 17−23.

(8) (a) Pratten, M. K.; Lloyd, J. B.; Hörpel, G.; Ringsdorf, H. *Makromol. Chem.* **1985**, *186*, 725−733. (b) Emmelius, M.; Hörpel, G.; Ringsdorf, H.; Schmidt, B. *Polym. Sci. Technol.* **1986**, *34*, 313−331.

(9) Cao, T.; Munk, P.; Ramireddy, C.; Tuzar, Z.; Webber, S. E. *Macromolecules* **1991**, *24*, 6300−6305.

(10) Allen, C.; Yu, Y.; Maysinger, D.; Eisenberg, A. *Bioconjugate Chem.* **1998**, *9*, 564−572.

(11) Kabanov, A. V.; Nazarova, I. R.; Astafieva, I. V.; Batrakova, E. V.; Alakhov, V. Y.; Yaroslavov, A. A.; Kabanov, V. A. *Macromolecules* **1995**, *28*, 2303−2314. Alakhov, V. Y.; Moskaleva, E. Y.; Batrakova, E. V.; Kabanov, A. V. *Bioconjugate Chem.* **1996**, *7*, 209−216.

(12) Zhang, L.; Yu, K.; Eisenberg, A. *Science* **1996**, *272*, 1777−1779. Savic, R.; Luo, L.; Eisenberg, A.; Maysinger, D. *Science* **2003**, *300*, 615−618.

(13) Discher, D. E.; Eisenberg, A. *Science*. **2002**, *297*, 967−973.

(14) Gabizon, A. A. *Cancer Res.* **1992**, *52*, 891−896. Paphadjopoulos, D.; Allen, T. M.; Gabizon, A.; Mayhew, E.; Matthay, K.; Huang, S. K.; Lee, K.-D.; Woodle, M. C.; Lasic, D. D.; Redemann, C.; Martin, F. J. *Proc. Natl. Acad. Sci.* **1991**, *88*, 11 460−11 464. Lasic, D. D.; Papahadjopoulos, D. *Science* **1995**, *267*, 1275−1276.

(15) Akiyoshi, K.; Kobayashi, S.; Shichibe, S.; Mix, D.; Baudys, M.; Kim, S. W.; Sunamoto, J. *J. Control. Release* **1998**, *54*, 313−320.

(16) Ribeiro, A. J.; Neufeld, R. J.; Arnaud, P.; Chaumeil, J. C. *Int. J. Pharm.* **1999**, *187*, 115−123.

(17) Cleland, J. L.; Lim, A.; Barrón, L.; Duenas, E. T.; Powell M. F. *J. Control. Release* **1997**, *47*, 135−150.

(18) Rilling, P.; Walter, T.; Pommershein, R.; Vogt, W. *J. Membrane Sci.* **1997**, *129*, 283−287.

(19) Birks, J. B. *Photophysics of Aromatic Molecules*; Wiley: New York, 1970; pp 301−371.

(20) Hynes, R. O. *Cell*, **1992**, *69*, 11−25. Yamada, K. M. *J. Biol. Chem.* **1991**, *266*, 12 809−12 812.

(21) (a) Pooga, M.; Hällbrink, M.; Zorko, M.; Langel, Ü. *FASEB* **1998**, *12*, 67−77. (b) Derossi, D.; Chassaing, G.; Prochiantz, A. *Trends Cell Biol.* **1998**, *8*, 84−87. (c) Pardridge, W. M.; Kumagai, A. K.; Eisenberg, J. B. *Biochem. Biophys. Res. Comm.* **1987**, *146*, 307−313.

(22) De Kruijff, B.; Cullis, P. R.; Radda, G. K. *Biochim. Biophys. Acta* **1975**, 406, 6−20.

(23) L'Heureux, G. P.; Fragata, M. *Biophys. Chem.* **1988**, *30*, 293−301.

(24) Szoka, F., Jr.; Papahadjopoulos, D. *Annu. Rev. Biophys. Bioeng.* **1980**, *9*, 467−508.

10^{-3} M for pyrene and 0.11 mg/mL (6.4×10^{-5} M) and 0.5 mg/mL (3.0×10^{-4} M) for the peptide to obtain the EAK01-PY and EAK05-PY solutions, respectively. These solutions, referred to as EAK-PY solutions, were kept on a stir plate until equilibrium was reached. Solutions containing pyrene were deemed at equilibrium when their fluorescence spectrum did not change with time anymore, which occurred after approximately 120 h.

Pyrene Transfer Experiments. The transfer of pyrene from the EAK-PY solutions into the EPC vesicles was monitored over time by fluorescence. For these experiments, aliquots (5−50 μL depending on the final pyrene concentration desired) of the EAK-PY solutions were mixed with 4 mL of a 7.4×10^{-4} M EPC solution in a 1×1 cm square cuvette inside the spectrofluorometer. The solution was stirred with a small magnetic stirrer. For each pyrene transfer experiment, an aliquot of the EAK-PY solution was deposited at the bottom of the quartz cuvette and it was mixed with the EPC solution. The amount of each solution was weighed before the cuvette was brought to the spectrofluorometer and the experiment was launched. The entire time needed to prepare the sample before initiating a time-dependent fluorescence measurement was less than 2 min.

Calibration Curve. Solutions of pyrene in EPC vesicles with pyrene concentrations ranging from 10^{-6} M to 10^{-4} M and an EPC concentration of 7.4×10^{-4} M were prepared by placing an appropriate amount of pyrene dissolved in THF into a 20 mL vial. The THF was evaporated under a stream of nitrogen to produce a film of pyrene at the bottom of the vial. The pyrene was then dissolved in 10 mL of vesicle solution, referred to as EPC-PY solutions. All solutions were kept on a magnetic stir plate for the duration of the experiments.

Dynamic Light Scattering Measurements. The hydrodynamic diameter of the vesicles was obtained on a Brookhaven BI-200 SM light scattering goniometer equipped with a Lexel 2 W argon ion laser operating at 514.5 nm. The refractive index and viscosity of water were taken to be 1.33 and 0.89 mPa·s, respectively. The sample cells were cleaned before each measurement by flushing them in an acetone fountain for 20 min. All measurements were performed at 25 °C at a measurement angle of 90°.

Steady-State Fluorescence Measurements. Fluorescence spectra were acquired on a Photon Technology International LS-100 fluorometer with a pulsed xenon lamp as the light source. The spectra of all solutions were obtained with a right angle configuration. A triangular fluorescence cell with a front-face arrangement was used to obtain the spectrum of the solid pyrene crystals. All samples were excited at 336 nm and the emission spectra were collected from 340 to 650 nm. The I_E/I_M ratio, where I_M and I_E represent the fluorescence intensities of the pyrene monomer and excimer, respectively, was obtained by taking the ratio of I_M measured by taking the integral under the fluorescence spectrum from 369 to 373 nm to I_E measured by taking the integral under the fluorescence spectrum from 500 to 530 nm.

The calibration curve required accurate fluorescence measurements carried out on different days on the pyrene monomer of the EPC-PY samples. To this effect, the emission intensity of the pyrene monomer for the EPC-PY solutions was monitored at 371 nm over a few minutes and averaged to yield I_M. To account for day-to-day lamp fluctuations, the intensity of a pyrene monomer standard (a sealed and degassed solution of pyrene in ethanol, $[PY] = 3.85 \times 10^{-5}$ M) was acquired at 371 nm and averaged over 2.5 min to yield I_S after each spectrum of the EPC-PY solutions. The corrected value of the monomer intensity (I_M/I_S) for the EPC-PY solutions was found by dividing I_M by I_S.

To obtain kinetic information for the transfer of pyrene from EAK to the EPC vesicles, the emission intensity of the pyrene monomer (I_M), was monitored at 371 nm, over a 4.0 h time span at 1 s intervals. If I_M did not reach a plateau after 4 h, then the solution was checked the next day (approximately 17−20 h later) for a 10 min time span. All solutions used for the transfer of pyrene from EAK to the EPC vesicles reached equilibrium after 17−20 h and day-to-day fluctuations were accounted for by dividing the fluorescence intensity of each I_M-versus-time profile by the average intensity of the standard (I_S). For each pyrene release experiment, I_M was recorded while constantly stirring the solution in the fluorometer.

Time-Resolved Fluorescence Measurements. Excimer fluorescence decay profiles were obtained with a Photochemical Research Associates Inc. System 2000 using the time-correlated single photon counting technique. The excitation wavelength was set at 335 nm and the fluorescence from the excimer was monitored at 510 nm. A filter was used with a cutoff of 495 nm to block potential light scattering leaking through the detection system. All decays were collected over 512 channels using a front-face geometry. A total of 20 000 counts were acquired at the peak maximum of the lamp and decay curves. The analyses of the decay curves were performed with the δ-pulse deconvolution. A reference decay curve of a degassed solution of BBOT [2,5-bis(5-*tert*-butyl-2-benzoxazolyl)thiophene] in ethanol ($\tau = 1.47$ ns)[25] was used for the analysis of the excimer decay curve. The excimer decays were fitted with a sum of three exponentials according to eq 1.

$$i_E(t) = a_{E1}\exp(-t/\tau_{E1}) + a_{E2}\exp(-t/\tau_{E2}) + a_{E3}\exp(-t/\tau_{E3}) \quad (1)$$

The parameters of the fit were optimized using the Marquardt−Levenberg algorithm.[26] The quality of the fits was established from the χ^2 (<1.30) values and the random distribution around zero of the residuals and of the autocorrelation function of the residuals.

Scanning Electronic Microscopy (SEM). LEO Elektronenmikroskopie field emission SEM (GmbH, Oberkochen, Germany) was used to study the morphology and dimension of the EAK-pyrene complexes. The SEM samples were prepared on the same day that the release experiments were conducted. An SEM sample was prepared by depositing 20 μL of an EAK-PY solution on a freshly cleaved mica surface, which was affixed on a SEM setup using a conductive carbon tape. The EAK-PY solution was allowed to settle for 10 min to ensure the adhesion of the complexes on the surface. It was then washed twice with a total of 400 μL pure water and air-dried overnight under a Petridish-cover to avoid any possible contamination before SEM imaging. The sample was coated with 20 nm gold prior to the

(25) Measured on Pr. M. A. Winnik (U. of Toronto, Canada) picosecond time-resolved fluorometer.
(26) Press, W. H.; Flannery, B. P.; Teukolsky, S. A.; Vetterling, W. T. *Numerical Receipes. The Art of Scientific Computing (Fortran Version)*; Cambridge University Press: Cambridge, 1992; pp 523−528.

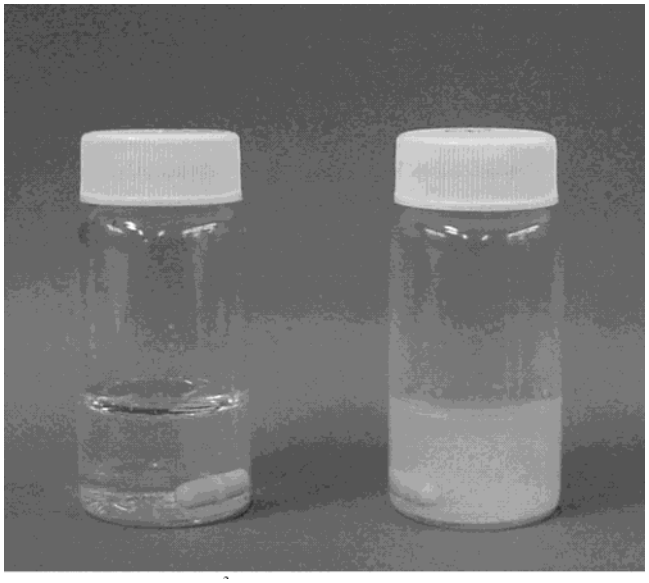

Figure 1. Pyrene crystals ([PY] = 5.3×10^{-3}M) in water (left) and with EAK ([PY] = 5.3×10^{-3}M, [EAK] = 3.0×10^{-4}M = 0.5 mg/mL) in aqueous solution (right) after stirring both solutions for 2.5 h.

scanning and the images were collected using the secondary electron (SE2) mode at 5 kV.

Results

Pyrene was chosen as a model hydrophobic compound since its solubility in water is very low. Its concentration in saturated aqueous solutions has been reported to be either 3.8×10^{-7} mol/L[27] or 7.0×10^{-7} mol/L.[28] In the presence of the EAK peptide, large amounts of pyrene (about 5×10^{-3} mol/L) can be stabilized in water via the adsorption of EAK onto the surface of pyrene microcrystals (Figure 1).[29] This phenomenon demonstrates the potential use of EAK as a carrier of hydrophobic compounds. To target the hydrophobic domains of a living cell, a hydrophobic compound must be delivered into the cell membrane. Because lipids constitute the essential element of cell membranes, EPC vesicles were prepared as a model membrane to monitor the transfer of pyrene from the EAK carrier into the lipid vesicles.

The size distribution of the prepared vesicles was determined by dynamic light scattering (Figure 2). The hydrodynamic diameter of the vesicles ranged from 70 to 130 nm with an average diameter of 95 nm. Literature reports state that vesicles prepared by sonication with a size range of 70−500 nm are defined as large unilamellar vesicles (LUVs).[30−32] Minute amounts of larger particles were observed in only a few samples (cf. Figure 2A). These larger particles could be due to the presence of either residual dust or large multilamellar vesicles. Control experiments were done to ensure that the addition of pyrene, alone or stabilized by EAK, to the vesicles did not affect their size. The size distribution of the vesicles mixed with pyrene and EAK was found to be virtually identical to that of the original EPC solution (Figure 2).

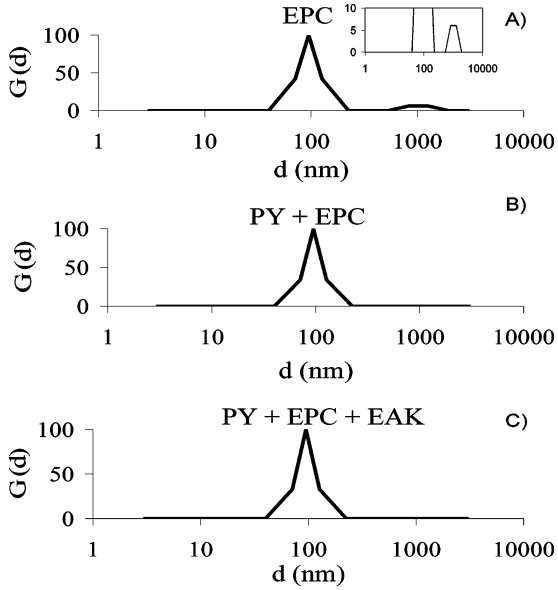

Figure 2. Dynamic light scattering for (A) EPC vesicles ([EPC] = 6.9×10^{-4}M). The inset shows the hump at 1000 nm to better visualize the larger vesicles; (B) pyrene in EPC vesicles ([PY] = 4.8×10^{-5}M, [EPC] = 6.9×10^{-4}M); and (C) EAK05−PY solution mixed with EPC vesicles ([PY] = 4.6×10^{-5}M, [EAK] = 2.8×10^{-6}M, [EPC] = 6.9×10^{-4}M).

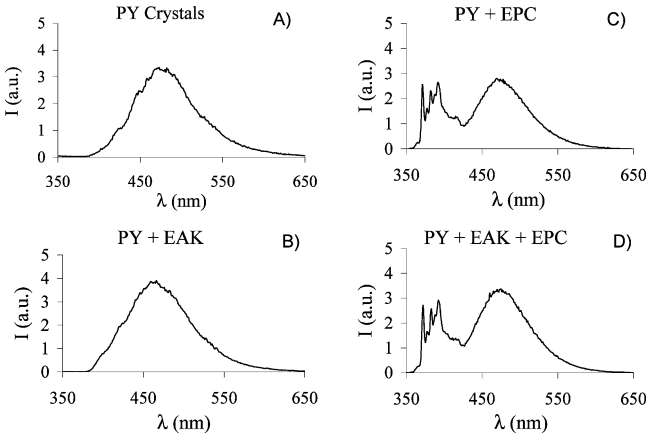

Figure 3. Steady-state fluorescence emission spectra of (A) solid pyrene crystals (front face geometry), (B) EAK05-PY solution ([PY] = 5.3×10^{-3} M, [EAK] = 3.0×10^{-4} M), (C) pyrene in EPC vesicles ([PY] = 4.8×10^{-5} M, [EPC] = 6.9×10^{-4} M), and (D) EAK-PY solution mixed with EPC vesicles ([PY] = 4.6×10^{-5} M, [EAK] = 2.8×10^{-6} M, [EPC] = 6.9×10^{-4} M), λ_{ex} = 336 nm.

Fluorescence spectra of the pyrene solutions at equilibrium were acquired. The steady-state fluorescence spectrum of an aliquot of the EAK05-PY solution mixed with the EPC vesicles was compared to that of pyrene in EPC vesicles, the EAK05-PY solution, and solid pyrene crystals (cf. Figure 3). The steady-state fluorescence spectra show that the pyrene crystals and the EAK05-PY solution both exhibit a large amount of excimer with no visible pyrene monomer emission. The steady-state fluorescence spectra for pyrene in EPC vesicles and the EAK05-PY solution mixed with the vesicles are similar, with I_E/I_M values of 0.65 and 0.70, respectively. The ratio of the intensities of the first (371 nm) and the third (382 nm) peaks of the pyrene monomer, I_1/I_3, was used to determine the polarity of the pyrene environment.[33] The I_1/I_3 ratio equals 1.7 in a polar solvent like

(27) Stepanek, M.; Krijtova, K.; Prochazka, K.; Teng, Y.; Webber, S. E.; Munk, P. *Acta Polym.* **1998**, *49*, 96−102.
(28) Yekta, A.; Xu, B.; Duhamel, J.; Adiwidjaja, H.; Winnik, M. A. *Macromolecules* **1995**, *28*, 956−966.
(29) Fung, S.-H.; Bezaire, J. A.; Hong, Y.; Duhamel, J.; Chen, P., 2003 in preparation.
(30) Davidson, W. S.; Rodrigueza, W. V.; Lund-Katz, S.; Johnson, W. J.; Rothblat, G. H.; Phillips, M. C. *J. Biol. Chem.* **1995**, *270*, 17 106−17 119.
(31) Huang, H.; Ball, J. M.; Billheimer, J. T.; Schroeder, F. *Biochem. J.* **1999**, 593−603.
(32) Ostro, M. J. *Liposomes*; Marcel Dekker: New York, 1983; p 28.

Scheme 1

$$\mathrm{PY} + h\nu \longrightarrow \mathrm{PY}^* + \mathrm{PY} \underset{k_{-i}}{\overset{k_{diff}(t)}{\rightleftharpoons}} \mathrm{E}^* \longleftarrow (\mathrm{PYPY}) + h\nu$$
$$\downarrow 1/\tau_M \qquad\qquad \downarrow 1/\tau_E$$

water, and takes lower values in apolar solvents. The I_1/I_3 values for pyrene in EPC vesicles and the EAK-PY solution mixed with the vesicles both equalled 1.1. This is in good agreement with published I_1/I_3 values of pyrene in lipid vesicles[23] and demonstrates that some pyrene from the EAK-PY solution is located inside the hydrophobic vesicle membrane and has been released from the EAK coating. Similar observations were made with the EAK01-PY solution (data not shown).

Since an active compound can exhibit higher activity when it is present in the crystalline form due to its higher local concentration in the crystal,[34] it is important to assess whether pyrene in an EAK-PY solution with and without EPC vesicles is present as molecules which are dispersed in the peptide matrix or close-packed inside a microcrystal coated by a peptide sheath. While the microenvironment of the pyrene monomer can be easily determined from the measurement of the I_1/I_3 ratio, the same task is much harder to accomplish for the pyrene excimer. Indeed the steady-state fluorescence spectrum of the pyrene excimer does not provide enough information to determine whether the excimer is formed via diffusion of dispersed pyrene molecules (PY in EPC vesicles, Figure 3C) or from preassociated pyrene molecules (PY crystals, Figure 3A). This is illustrated in Scheme 1 where the excimer is shown to be produced via two pathways. The pyrene excimer can be formed either via diffusional encounters between pyrene molecules or from the direct excitation of pyrene dimers (PYPY). In Scheme 1, $k_{diff}(t)$ represents the time-dependent "rate constant" for excimer formation via diffusion, and τ_M and τ_E are the lifetimes of the pyrene monomer and excimer, respectively.[35]

To determine whether the pyrene excimer is formed via diffusional encounters or from direct excitation of a pyrene dimer, additional experiments must be performed. Time-resolved fluorescence decay measurements were carried out on the pyrene excimer of all samples shown in Figure 3. The results are shown in Figure 4. All the excimer fluorescence decays exhibited a rise time, but the magnitude of the rise time and the time scale of the decays are different. These differences are quantified by carrying out a triexponential fit according to eq 1. The parameters retrieved from the fits are listed in Table 1. Their values are discussed in order to establish the state of pyrene in the EAK-PY solution with and without EPC vesicles.

The rise time of the pyrene excimer formed in the pyrene crystals and in the EAK05-PY solution is short and equals 8.2 $\pm$ 0.4 ns. Two exponentials were required to fit the rise time of the pyrene excimer for the samples of pyrene in EPC vesicles and the EAK05-PY solution mixed with EPC vesicles. The rise time τ_2 has the heaviest contribution ($a_1/(a_1 + a_2) = 0.93$) and equals 41 $\pm$ 2 ns. This value is five times larger than the 8.2 ns rise time obtained for the pyrene crystals and the EAK05-PY solution.

The presence of EPC vesicles also lengthens the decay of the pyrene excimer. The second exponential with the pre-exponential factor a_2 exhibits the strongest contribution of the excimer decays for the pyrene crystals and the EAK05-PY solution. Its associated decay time equals 22 $\pm$ 0 ns. The third exponential with the pre-exponential factor a_3 represents the contribution of the excimer decay for the samples of pyrene in EPC vesicles and the EAK05-PY solution mixed with EPC vesicles. Its associated decay time equals 64 $\pm$ 2 ns, three times larger than that of the pyrene crystals and the EAK05-PY solution.

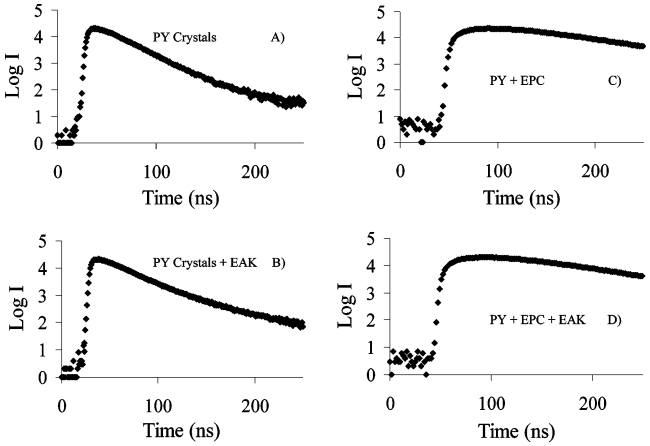

Figure 4. Fluorescence decays of the pyrene excimer for (A) solid pyrene crystals, (B) EAK05-PY solution ([PY] = 5.3×10^{-3} M, [EAK] = 3.0×10^{-4} M), (C) pyrene in EPC vesicles ([PY] = 4.8×10^{-5} M, [EPC] = 6.9×10^{-4} M), and (D) EAK05−PY solution mixed with EPC vesicles ([PY] = 4.6×10^{-5} M, [EAK] = 2.8×10^{-6} M, [EPC] = 6.9×10^{-4} M), λ_{ex} = 335 nm, λ_{em} = 510 nm. The decays shown in Figure 4C,D were acquired and analyzed over 500 ns, but they are truncated in Figure 4C,D to allow easier comparison with Figure 4A,B.

In Table 1, the negative pre-exponential factors obtained from the fits of the fluorescence decays are associated with the rise and the positive ones with the decay. Taking the ratio (ξ) of the sum of the negative pre-exponential factors over that of the positive pre-exponential factors ($\xi = a_-/a_+$) gives information about the process by which the excimer is being formed.[36,37] When the ξ ratio equals −1.0, no ground-state dimers are present in the solution and the excimers are formed via diffusion only. If ξ is more positive than −1.0, then ground-state dimers are present. Intuitively ground-state dimers should be present in the pyrene crystals since pyrene molecules are packed close to one-another, but few should be observed in the samples made with EPC vesicles, since the vesicle membranes should provide enough hydrophobic medium to dissolve pyrene. This is indeed observed. The pyrene crystals and the EAK05-PY solution yielded a ξ ratio equal to −0.55± 0.01. The samples of pyrene in EPC vesicles and the EAK05-PY solution mixed with EPC vesicles yielded a ξ ratio equal to −0.97± 0.01, very close to −1.00.

Comparison of the decays displayed in Figure 4 and the data listed in Table 1 leads to the conclusion that the excimers formed by the pyrene crystals and the EAK05-PY solution are similar to one another, just as those formed by the samples of pyrene in EPC vesicles and the EAK05-PY solution mixed with EPC vesicles are comparable. The analysis of the excimer fluorescence decays combined with that of the steady-state fluorescence

(33) Kalyanasundaram, K.; Thomas, J. K. *J. Am. Chem. Soc.* **1977**, *99*, 2039−2044.
(34) Jin, W.; Shi, X.; Caruso, F. *J. Am. Chem. Soc.* **2001**, *123*, 8121−8122.
(35) Duhamel, J.; Winnik, M. A.; Baros, F.; André, J. C.; Martinho, J. M. G. *J. Phys. Chem.* **1992**, *96*, 9805−9810.
(36) Prazeres, T. J. V.; Beingessner, R.; Duhamel, J.; Olesen, K.; Shay, G.; Bassett, D. R. *Macromolecules* **2001**, *34*, 7876−7884.
(37) Jones, A. S.; Dickson, T. J.; Wilson, B. E.; Duhamel, J. *Macromolecules* **1999**, *32*, 2956−2961.

Table 1. Parameters Obtained from the Analysis of the Fluorescence Decays of the pyrene excimer (λ_{ex} = 335 nm and λ_{em} = 510 nm)

	τ_1 (ns)	a_1	τ_2 (ns)	a_2	τ_3 (ns)	a_3	$a_1/(a_2+a_3)$	$(a_1+a_2)/a_3$	χ^2
PY crystals	8.6	−0.57	22	1.00	130	<0.01	−0.57		1.01
PY + EAK	7.8	−0.59	22	1.00	43	0.18	−0.54		1.05
PY + EPC	12	−0.08	40	−1.00	66	1.10		−0.96	0.92
PY + EPC + EAK	13	−0.08	43	−1.00	63	1.10		−0.97	1.21

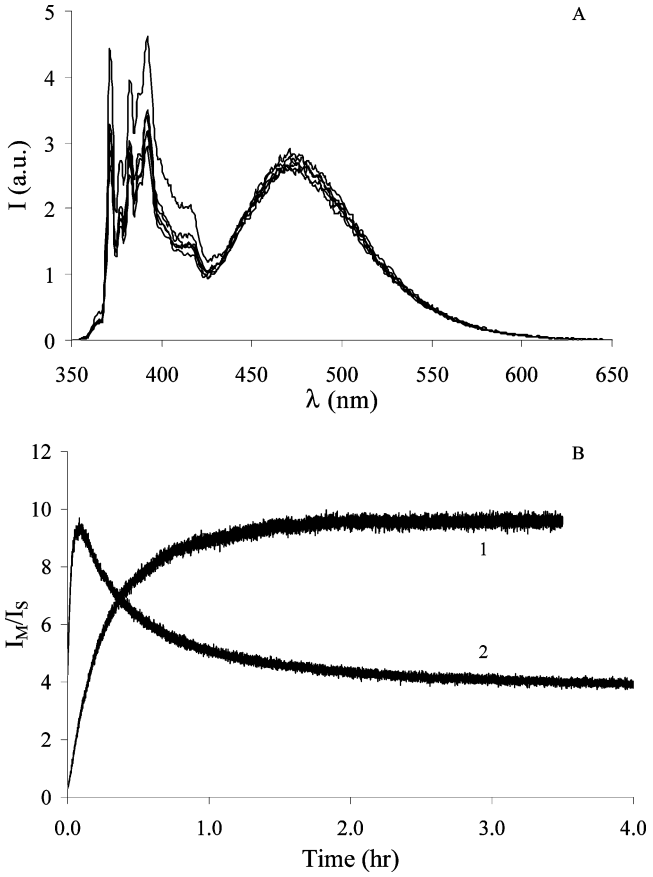

Figure 5. Fluorescence followed as a function of time for release of pyrene from its EAK coating into EPC vesicles, λ_{ex} = 336 nm: (A) Steady-state fluorescence emission spectra acquired at 0.25, 0.75, 1.1, 2.8, 3.8, and 5.1 h after solution preparation ([PY] = 4.6×10^{-5} M, [EAK] = 2.6×10^{-6} M, [EPC] = 6.9×10^{-4} M). (B) Fluorescence emission of the pyrene monomer when different amounts of EAK01-PY solution are added to EPC. λ_{em} = 371 nm. The fluorescence intensity (I_M) is divided by that of the standard (I_S). Profile (1) Data acquisition over a 3.4 h time span with 1s intervals ([PY] = 1.5×10^{-5} M, [EAK] = 1.9×10^{-7} M, [EPC] = 7.4×10^{-4} M). Profile (2) Data acquisition over a 4 h time span with 1s intervals ([PY] = 10×10^{-5} M, [EAK] = 1.3×10^{-6} M, [EPC] = 7.4×10^{-4} M).

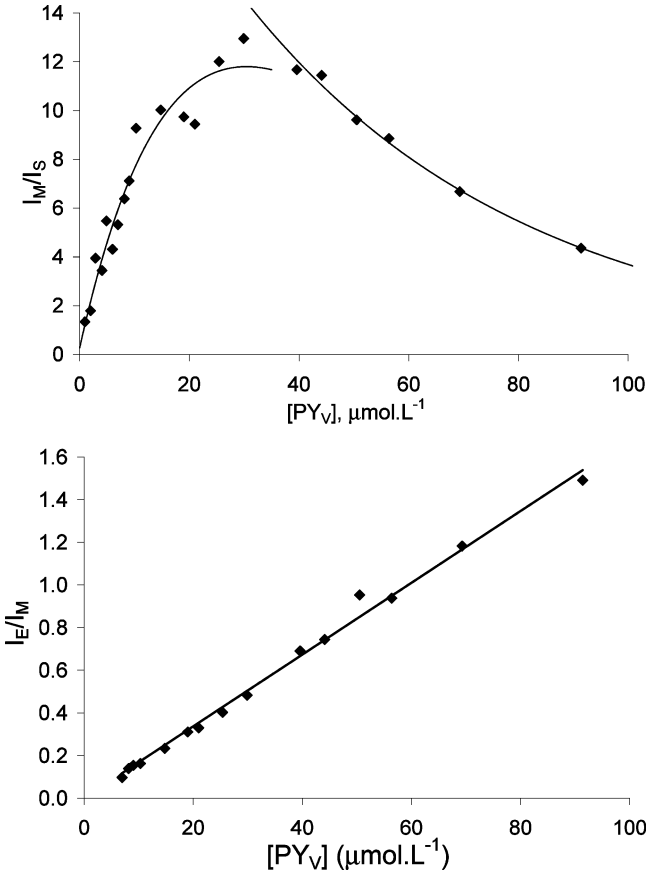

Figure 6. Calibration curve for different pyrene concentrations in EPC vesicles ([EPC] = 7.4×10^{-4} M). The concentration of pyrene ranged from 10^{-6} M to 100×10^{-6} M. The fluorescence intensity (I_M) is divided by that of the standard (I_S). (Top panel) Up to [PY] = 25×10^{-6} M, the monomer intensity was well-fit with a biexponential, $I_M = -99e^{-36000\times[PY]} + 102e^{-25000\times[PY]} - 2.4$. For higher concentrations, a single exponential was used to fit the I_M versus [PY] profile, $I_M = 26e^{-20000\times[PY]}$. (Bottom panel) Ratio of the excimer-to-monomer intensities obtained for different pyrene concentrations.

spectra leads to the following conclusions: Pyrene in the EAK05-PY solution is in a crystalline form (comparison of Figure 3A with Figure 3B, and of Figure 4A and Figure 4B). Adding EAK to the pyrene crystals under vigorous stirring yields a stable dispersion of smaller pyrene crystals (a few micrometers in radius,[29] cf. Figure 9) which are stabilized in solution via the adsorption of EAK onto their surface. Mixing the EAK05-PY solution with the EPC vesicles yields a solution where pyrene is molecularly dissolved inside the vesicle membrane. This is clearly visible from the ratio I_1/I_3 of the pyrene monomer which equals that found for pyrene in EPC vesicles. The monomer-to-excimer ratio, I_E/I_M, is equal within experimental error, whether the EPC vesicles are loaded with pyrene by placing the EPC solution in a flask at the bottom of which a thin film of pyrene has been prepared (Figure 3C) or by mixing the EPC solution with the EAK-PY solution (Figure 3D). Finally, very few pyrene crystals of the EAK-PY solution are expected to remain after mixing with the EPC vesicles has been completed. If some pyrene crystals were still present, the ξ ratio would take a more positive value than −0.97 (cf. Table 1). Observations similar to those reported for EAK05-PY in Figures 3 and 4 were made with the EAK01-PY solution.

All excimer decays required three exponentials in order to obtain satisfying fits and the ξ ratio was substantially more positive than −1.00 for the fluorescence decays of the pyrene crystals and the EAK-PY solution. These results stand at odd with the biexponential behavior expected by the well-established Birks' scheme for the pyrene excimer decays.[19] The Birks' scheme predicts that in low viscosity organic solvents (η < 1 mPa.s), where no ground-state pyrene dimers exist, the excimer

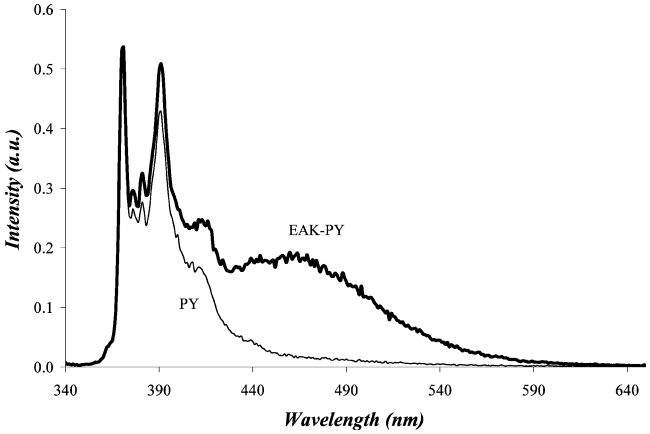

Figure 7. Fluorescence spectra ($\lambda_{ex} = 336$ nm) of buffer solutions saturated with pyrene (−), [PY] $\sim 7 \times 10^{-7}$ M) and of EAK-PY solution (−, [PY] $\sim 4.4 \times 10^{-5}$ M).

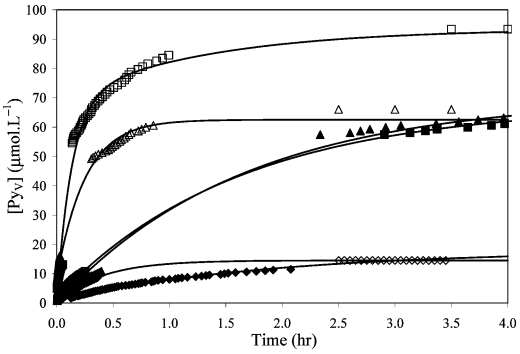

Figure 8. Fluorescence versus time profiles for the release of molecular pyrene from pyrene microcrystals encapsulated in an EAK coating into a solution of EPC liposomes ([EPC] $= 7.4 \times 10^{-4}$ M). Hollow and solid symbols are for pyrene transfer experiments carried out with EAK01-PY and EAK05-PY, respectively. The final pyrene concentrations are as follows: (□) [Py] $= 9.3 \times 10^{-5}$ M; (△) [Py] $= 6.6 \times 10^{-5}$ M; (◇) [Py] $= 1.45 \times 10^{-5}$ M; (■) [Py] $= 6.5 \times 10^{-5}$ M (from settled EAK05-PY solution); (▲) [Py] $= 6.8 \times 10^{-5}$ M; (◆) [Py] $= 1.8 \times 10^{-5}$ M. All release experiments reported in Figure 8 were carried out with the same batch of EAK and the same stock solution of EPC lipid used in the calibration curve shown in Figure 6.

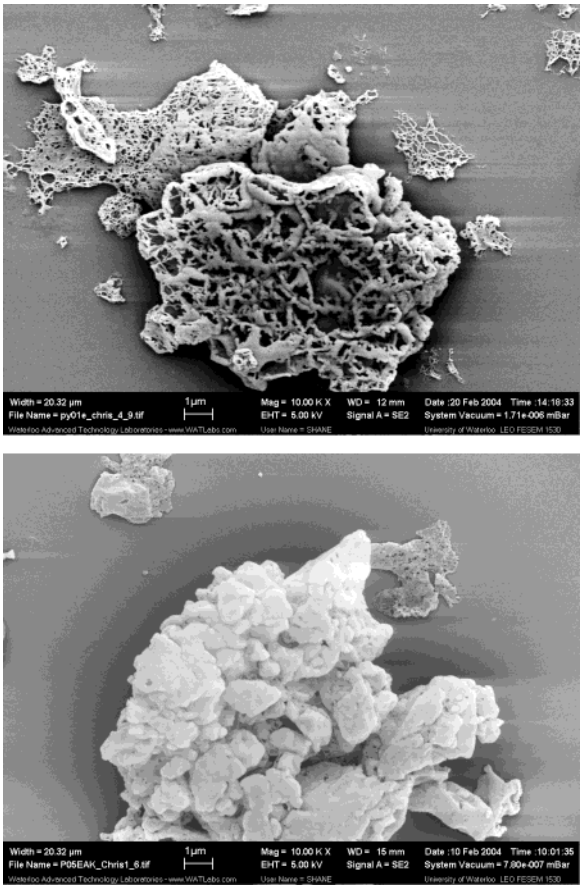

Figure 9. Scanning electron micrographs of the pyrene crystals of the EAK01-PY solution (top) and the EAK05-PY solution (bottom).

fluorescence decays can be fitted with two exponentials and the ξ ratio equals −1.00. However these ideal conditions are not obtained with the systems studied in this work. In the case of pyrene dissolved inside the membrane of EPC vesicles, pyrene experiences a viscous environment ($\eta > 1$ mPa.s) which leads to transient effects. The rate constant for excimer formation $k_{diff}(t)$ shown in Scheme 1 becomes time-dependent. These transient effects are usually observed in the early portion of the fluorescence decay (first exponential) resulting in the need of a third exponential to properly fit the fluorescence decay.[35]

In the case of the pyrene crystals and the EAK-PY solutions, the pyrene molecules are held together via internal crystal packing forces. Since no diffusion takes place inside the crystals, the Birks' scheme becomes irrelevant. The surprising outcome of the analysis of the excimer fluorescence decays is not that the ξ ratio is more positive than −1.00, but rather that it does not equal zero as expected for the fluorescence emission of pyrene dimers found in the pyrene crystal. This is certainly due to the geometry adopted by the pyrene molecules in the crystal, which is not the optimal one to form an excimer. The energy requirements to obtain an excimer configuration are different from those which hold two pyrene molecules inside a pyrene crystal. Upon UV irradiation of a pyrene crystal, the pyrene monomer absorbs a photon and is excited. Its energy can be transferred to nearby pyrene via energy hopping until a ground-state dimer is reached. The pyrene dimer allows for the formation of an excimer which represents an energy sink in the crystal matrix. The energy hopping mechanism induces a delay in the process of excimer formation and explains the rise time observed in the fluorescence decays. Direct excitation of the crystal defects leads to the instantaneous formation of an excimer so that the ξ ratio is more positive than −1.00. A similar behavior has been reported for the naphthalene excimer fluorescence of poly(ethylene-2,6-naphthalene dicarboxylate).[37]

Steady-state fluorescence spectra were acquired over time to observe the transfer of pyrene from the colloidal pyrene crystals stabilized by EAK in aqueous solution into the EPC vesicles. First the spectra were obtained shortly after sample preparation at various time intervals over a total period of 5 h (Figure 5A). For each spectrum, the I_1/I_3 ratio equals 1.1 indicating that the pyrene monomer is always located inside the hydrophobic vesicle membrane. Initially, the monomer intensity is seen to decrease rapidly, but after 0.75 h, little change is observed in the fluorescence spectra. To probe the pyrene transfer during the first hour more precisely, the monomer intensity was monitored as a function of time over a period of 4 h with 1 s intervals at an emission wavelength of 371 nm. Two profiles are shown in Figure 5B. Profiles 1 and 2 represent the release of pyrene into EPC vesicles when different amounts of EAK01-PY solution are added to the EPC solution, leading to final pyrene concentrations of 1.5×10^{-5} M and 10×10^{-5} M,

respectively. Profile 1 in Figure 5B obtained at low pyrene concentration exhibits a continuous increase of I_M with time during the first hour and reaches a plateau after close to 2 h. Profile 2 obtained at higher pyrene concentration shows a rapid increase in I_M with time going through a maximum after 7 min, followed by a continuous decrease down to a plateau reached after about 3 h.

Quantitative analysis of I_M-versus-time profiles such as those shown in Figures 5B is complicated by fluorescence artifacts, which are associated with the transition undergone by pyrene from a crystal (initial state = pyrene microcrystals of the EAK-PY solution) to individual molecules dissolved inside the vesicle membrane (final state = EAK-PY solution mixed with EPC vesicles). Inside a pyrene crystal where many pyrene molecules are close-packed, the probability of pyrene to absorb a photon is much smaller than when an equal number of pyrene molecules are molecularly dissolved inside the vesicle. This statement can be demonstrated in the following manner. Assuming the extinction coefficient of 54 000 $M^{-1}\cdot cm^{-1}$ of pyrene in cyclohexane at 336 nm[38] for pyrene molecules located inside a pyrene crystal and a density of 1 $g\cdot cm^{-3}$ for the pyrene microcrystals, and using the 202 $g\cdot mol^{-1}$ molar mass of pyrene and the 10 μm size of a pyrene microcrystal coated with EAK (cf. Figure 9) as the path length (10 $\mu m = 10^{-3}$ cm), such a particle would have an absorption of 267! Consequently, most of the pyrene molecules located inside a 10 μm-large pyrene microcrystal cannot absorb any light. This can be referred to as a peculiar inner filter effect which is the result of the aggregation of numerous absorbing species into larger units. The overall absorption of the EAK-PY solutions is lower than anticipated from the actual pyrene concentration. By spreading over a larger volume, the molecularly dissolved pyrene increases its chances to absorb a photon. As the pyrene crystals dissolve, the pyrene absorption increases and so does the fluorescence of the pyrene monomer. As shown in the Profile 1 of Figure 5B, I_M reaches a plateau when all the pyrene is molecularly dissolved inside the vesicles. If the amount of the EAK-PY solution added to the liposome solution is too large, then the dissolution of pyrene molecules in the lipid vesicles leads to too large a pyrene absorption. The inner filter effect[39] takes place and the fluorescence of the pyrene monomer decreases until the crystals are fully dissolved and a plateau is reached. This is observed in Figure 5B for Profile 2 where the final pyrene concentration is 5.6 times larger than that of Profile 1.

Several other factors could affect the I_M-versus-time profiles shown in Figure 5B such as multiple scattering with the EPC liposomes and pyrene microcrystals as scatterers, or potential quenching of the pyrene monomer dissolved inside the lipid vesicle by the pyrene microcrystals. Although pyrene microcrystals could act as quenchers, it must be noted that the pyrene crystals are very large, being often larger than the EPC vesicles (cf. Figure 9). Consequently, they are expected to be static with respect to the pyrene molecules dissolved in the lipid bilayer and quenching of the pyrene monomer is more likely to occur via diffusional encounter with another fast moving pyrene monomer dissolved in the liposome. Multiple scattering might also be present, but it would be expected to occur also with the liposome solutions which are used in the calibration curve (cf. Figure 6A) for analyzing the profiles shown in Figure 5B in a quantitative manner. Consequently, by using the same liposome solutions for the calibration curve and the release experiments, such artifacts are expected to be much reduced.

While the fluorescence behavior of the pyrene monomer shown in Figure 5B is relatively straightforward to explain, the behavior of the excimer fluorescence is more complicated. This is because the excimer is formed from two different pathways (cf. Scheme 1), either via the direct excitation of pyrene crystals or via diffusional encounters between an excited pyrene and a ground-state pyrene, both molecularly dissolved inside the vesicle membrane. On one hand, as the pyrene crystals dissolve, the molecularly separated pyrenes must diffusionally encounter to form excimer, a less efficient process for excimer formation. On the other hand, the pyrene molecules dissolved inside the vesicle membrane capture more photons leading to the excitation of more pyrene monomers which results in the formation of more excimer inside the membrane. The overall balance between these two effects is difficult to quantify and the I_E-versus-time profiles are not reported for the excimer.

To obtain quantitative information from the fluorescence data, the fluorescence intensity of the pyrene monomer dissolving inside the vesicle membrane shown in Figure 5B was compared to that of standard solutions. A series of solutions was prepared containing a fixed amount of EPC ([EPC] = 7.4×10^{-4} M) with pyrene concentrations ranging from 1×10^{-6} up to 100×10^{-6} M. The fluorescence intensity of the pyrene monomer divided by that of the standard to account for lamp fluctuations (I_M/I_S) is shown as a function of pyrene concentration in Figure 6A. The inner filter effect is clearly visible in the concentration profile of I_M (Figure 6A). As the pyrene concentration increases from zero, more pyrene molecules are present in solution and the fluorescence intensity increases. At a pyrene concentration of $30(\pm 10) \times 10^{-6}$ M, I_M passes through a maximum. The absorption becomes too large and the inner filter effect leads to a decrease of the fluorescence intensity upon further increase in pyrene concentration. It must be noted that, despite increased excimer formation, the pyrene monomer fluorescence intensity always increases with pyrene concentration when excimer formation occurs by diffusion. Thus, the decrease of I_M for pyrene concentrations larger than 40×10^{-6} M cannot be due to enhanced excimer formation, and can only be accounted for by invoking the inner filter effect.

The ratio I_E/I_M shown in Figure 6B is not affected by the inner filter effect because the inner filter effect reduces the intensity of the entire fluorescence spectrum by the same proportion. Consequently, taking the ratio of two fluorescence intensities obtained from the same fluorescence spectrum cancels out the inner filter effect. The ratio I_E/I_M increases linearly with pyrene concentration in Figure 6B. This trend is typical for an excimer being formed via a diffusion-controlled process,[19] an expected result for the formation of pyrene excimer inside a lipid membrane. This result agrees also with the analysis of the excimer fluorescence decays for pyrene in EPC vesicles and the EAK-PY solutions mixed with EPC vesicles, which were carried out at the end of each release experiment and which all yielded a ξ ratio of the pre-exponential factors larger than -0.95, a value very close to -1.00 as expected for an excimer formed by a diffusion-controlled process.

(38) Berlman, I. B. *Handbook of Fluorescence Spectra of Aromatic Molecules*; Academic Press: New York, 1971; p 383.
(39) Lakowicz, J. R. *Principles of Fluorescence Spectroscopy*; Plenum Press: New York, 1983; pp 44−45.

Table 2. Rates of Transfer of Molecular Pyrene from Pyrene Microcrystals Encapsulated in an EAK Coating into a Solution of EPC Liposomes

[Py], μmol·L^{-1}	[EAK] = 0.1 mg/mL	[EAK] = 0.5 mg/mL
15	$k_{trans} = 2.5 \pm 0.2$ h^{-1}	
66	$k_{trans} = 4.0 \pm 0.1$ h^{-1}	
93[a]	k_{trans} (fast) $= 7.6 \pm 0.3$ h^{-1} (63%) k_{trans} (slow) $= 0.8 \pm 0.1$ h^{-1} (27%)	
18		$k_{trans} = 0.52 \pm 0.03$ h^{-1}
65 (from settled EAK05-PY solution)		$k_{trans} = 0.60 \pm 0.02$ h^{-1}
68		$k_{trans} = 0.62 \pm 0.02$ h^{-1}

[a] Two exponentials were needed to fit the release profile according to the equation:

$$[Py_V]_{(t)} = [Py]_{(t=\infty)} \times [1 - a_{fast} \times \exp(-k_{trans}^{fast} t) - a_{slow} \times \exp(-k_{trans}^{slow} t)]$$

where $a_{slow} + a_{fast} = 1.0$.

Interestingly, the presence of pyrene crystals in the EAK-PY sample is not expected to affect the fluorescence of the pyrene monomer at the pyrene concentration used in the mixing experiments. This can be demonstrated by comparing the fluorescence intensity of aqueous solutions saturated with pyrene ($\sim 7 \times 10^{-7}$ M) with that of an EAK05-PY sample with a pyrene concentration of 4.4×10^{-5} M. Figure 7 exhibits the fluorescence emission of the pyrene monomer in water for the EAK05-PY sample. The pyrene molecules of the EAK05-PY sample which are not solubilized in water form pyrene microcrystals stabilized by EAK. Nevertheless, the fluorescence signal of the pyrene monomer of the EAK05-PY sample is not affected by the high pyrene concentration in the EAK05-PY solution. This is a consequence of the presence of microcrystals whose large dimensions do not allow the pyrenes located at the core to absorb the excitation light. The main result is that whereas molecular pyrene induces a strong inner filter effect at a concentration of 4.4×10^{-5} M (cf. Figure 6A), pyrene crystals do not do this at the same pyrene concentration (cf. Figure 7).

The fluorescence intensity of standard solutions containing pyrene and EPC vesicles has been carefully calibrated in Figure 6. These results can now be used to analyze the fluorescence intensity profiles such as those reported in Figures 5B in order to determine the time-dependent concentration profile of pyrene being incorporated inside the EPC vesicle membrane. While the pyrene crystals stabilized by EAK dissolve and molecular pyrene is transferred to the EPC vesicles, the pyrene monomer and excimer are clearly identifiable in the fluorescence spectra (cf. Figure 5A). However, the excimer is formed inside the pyrene crystals and the EPC vesicle membrane, whereas the monomer is found uniquely inside the hydrophobic vesicle wall. In other words, the fluorescence signal arising from the pyrene excimer has two sources, whereas that of the pyrene monomer has only one (cf. Scheme 1). Consequently the pyrene concentration present inside the vesicle was determined by comparing the fluorescence intensity of the pyrene monomer obtained as a function of time in release profiles such as those shown in Figure 5B with that shown in Figure 6A as a function of pyrene concentration. In doing so, a time-dependent concentration profile could be determined for pyrene located inside the vesicles.

At different times, the fluorescence signal obtained in release experiments such as the ones shown in Figure 5B was compared to that of Figure 6A and a pyrene concentration was found. The results of the pyrene release experiments are shown in Figure 8. This procedure works well when the fluorescence intensity of the monomer (I_M) shown in Figure 6A varies with the pyrene concentration. However Figure 6A shows that I_M passes through a maximum, and that its value varies little for pyrene concentration between 1.5×10^{-5} and 5.0×10^{-5} M. Consequently as the fluorescence intensity approaches its maximum value in Figure 5B, the associated pyrene concentration can take any value between 1.5×10^{-5} and 5.0×10^{-5} M. This is why a gap is observed in Figure 8, where no data points have been reported for pyrene concentrations ranging from 1.5×10^{-5} to 5.0×10^{-5} M. Despite this procedural defect, the trends shown in Figure 8 are clear. As time elapses, more pyrene is being transferred from the pyrene crystals into the EPC vesicles. Yet, for similar final pyrene concentrations in the EPC vesicles, the release of pyrene from the EAK coated pyrene crystals appears to occur much more slowly for the EAK05-PY solution than for the EAK01-PY solution.

Several pathways can be suggested to describe the transfer of pyrene from the pyrene crystals coated with EAK into the EPC vesicles. Consequently, it becomes difficult to establish the uniqueness of a model describing the transfer. However the trend shown in Figure 8 can be fit with eq 2 which suggests that a single rate constant k_{trans} can handle the overall transfer of pyrene.

$$[PY_V](t) = [PY_V]_{eq} - ([PY_V]_{eq} - [PY_V]_0) \exp(-k_{trans} \times t) \quad (2)$$

In eq 2, $[PY_V](t)$, $[PY_V]_{eq}$, and $[PY_V]_0$, represent the pyrene concentration inside the vesicles at time t, at equilibrium (infinite time), and at time $t = 0$ s, respectively. The fit of the data with eq 2 is shown in Figure 8. The corresponding rate constants of release are listed in Table 2.

The rate constants of release listed in Table 2 report the same effect shown in Figure 8, namely that the release of pyrene from pyrene crystals coated with EAK proceeds in a much slower manner when a higher molecular ratio of EAK-to-pyrene is used. Intuitively one would expect that for the same amount of colloidal material (i.e., the pyrene crystals), the use of a larger amount of colloidal stabilizer (i.e., EAK) would yield smaller colloidal particles, whose higher surface area would induce a faster release into the EPC vesicles. The opposite effect is observed. This phenomenon could be due to a thicker coating of the pyrene crystals when a higher EAK concentration is being used. If the EAK coating were to prevent the release of pyrene from the pyrene crystals, then a higher molecular ratio of EAK-to-pyrene would yield a thicker coating of the crystals and a slower rate of release, as observed.

If this explanation were correct, then the coating of the pyrene crystals should exhibit different features whether a molecular

ratio of pyrene-to-petpide of 78 or 16 was used such as the ones used for EAK01-PY and EAK05-PY, respectively. SEM pictures were acquired for the EAK01-PY and EAK05-PY solutions. As shown in Figure 9, the surfaces of the pyrene crystals exhibited very different appearances depending on the peptide-to-pyrene ratio. Pyrene crystals imaged from the EAK01-PY solution display elaborate lace-like features, whereas most of the pyrene crystals imaged from the EAK05-PY solution appeared to be wrapped in a thick coating. The micrographs shown in Figure 9 suggest that higher peptide-to-pyrene molecular ratios lead to the formation of a thick coating which inhibits the release of pyrene. When lower peptide-to-pyrene ratios are utilized, the interaction of pyrene and EAK yields lace-like structures which facilitate the release of pyrene into the vesicles.

Without continuous stirring, the EAK-PY colloidal suspensions were found to settle over time. To investigate whether the settling of the colloids produced by the interactions of EAK with pyrene had an effect on the rate of pyrene release, a release experiment was performed where the EAK05-PY was allowed to settle over a period of 3 d. Then the EAK05-PY solution was shaken vigorously and a release experiment was conducted with the resuspended solution. The result is shown in Figure 8 and in Table 2. Within experimental error, no difference was observed in the release profiles whether the release experiment was performed with the settled or continuously stirred EAK05-PY solution.

Discussion

"Classic" carriers of hydrophobic compounds such as block copolymer micelles[7−12] and vesicles,[13] liposomes,[8b,14] and gel micro-encapsulations[15−18] provide sufficiently large hydrophobic microdomains to incorporate a hydrophobic compound. By contrast, EAK does not generate a matrix into which the hydrophobic compound pyrene is incorporated, but rather acts as a stabilizer which interacts with the surface of pyrene microcrystals and maintains them in solution. When the EAK-PY solution is mixed with EPC vesicles, pyrene is transferred from the pyrene crystals into the vesicle membrane until all pyrene crystals have disappeared. Inside the vesicle membrane, pyrene is molecularly dissolved and our fluorescence experiments did not indicate that any pyrene microcrystals remain.

The ionic character of EAK and its ability to self-assemble into fibrils composed of ion-paired β-sheets[1−3] suggest that EAK could adsorb onto the pyrene microcrystal surface in a manner similar to the layer-by-layer entrapment of microcrystals of hydrophobic compounds performed by adsorbing alternatively on their surface several layers of oppositely charged polyions.[40] In the case of layer-by-layer entrapment, successive adsorptions of oppositely charged polyions onto the surface of microcrystals yields microcrystals coated by a polymer matrix hosting ion pairs. Similarly, the pyrene microcrystals stabilized by EAK are surrounded by a peptide matrix held together by ion pairs. One difference between the two systems resides in the fact that EAK bears an equal number of positive and negative charges and the solution of stabilized microcrystals is prepared in one batch, whereas the polyions bear one type of charge (positive or negative) and they are added sequentially to the solution.

Dealing with crystalline colloids surrounded by a thin matrix of stabilizing material has the advantage of maximizing the density of the delivery system with respect to the cargo, which, in principle, should allow the carrier to deliver a lethal blow to a given target upon encounter. In a dramatic example, Caruso et al.[34] demonstrated that the encapsulation of catalase enzyme crystals by the alternate adsorption of poly(styrenesulfonate) and poly(allylamine hydrochloride) leads to 50 times higher biocatalytic activities than when the enzyme is molecularly solubilized in the polymeric film. Crystals of dyes (pyrene and fluorescein),[41a] drugs (ibuprofen),[41b] and proteins (lactase and catalase)[41c] can be successfully stabilized in aqueous solution by coating them with alternating layers of polyanions and polycations. Poly(allylamine hydrochloride), poly(diallyldimethylammonium chloride), poly(4-vinylpyridine), polysaccharides, and poly(sodium 4-styrenesulfonate) are typical examples of the polyions used to encapsulate the crystals. The present study demonstrates that the sapeptide EAK displays the same ability at coating microcrystals of hydrophobic compounds as the polyions used in the layer-by-layer entrapment technique, but also offers the additional feature of being biocompatible.[2]

One important advantage of the layer-by-layer entrapment techniques is the ability to control the wall thickness surrounding the cargo, and consequently, the rate of release. Slower rates of release have been observed when thicker coatings of poly(allylamine) and poly(sodium 4-styrenesulfonate) were applied onto pyrene or fluorescein diacetate microcrystals.[41a] Similarly, thicker peptide coating such as the one displayed in Figure 9 (bottom) led to a reduction of the rate of pyrene transfer. This feature bears the promise of controlling the rate of release of a hydrophobic cargo into a lipid bilayer by simply tuning the peptide-to-hydrophobic cargo molecular ratio.

Although pyrene has often been used as a model hydrophobic compound, we are not aware of any report in the literature where the rate of transfer of pyrene has been determined quantitatively from a delivery system to lipid vesicles. Often the carrier loaded with pyrene is either exposed to a less polar solvent like ethanol[41a−b] and the rate of pyrene release is measured, or to empty carriers and the rate of pyrene exchange between carriers is measured,[9,42] or the loaded carrier is kept in a dialysis bag and the rate of release of pyrene to the aqueous environment is monitored over time.[43] Such measurements only provide qualitative information about the rate of release of pyrene from a given carrier, which makes it difficult to compare the value of the transfer rate constant k_{trans} obtained in this study with that obtained for other delivery systems.[7b−c,9−11,41a−b,43] However, we believe that the procedure used in this work presents several advantages. First, lipids are an essential component of cell membranes and the use of lipid vesicles as the recipients of the hydrophobic pyrene encapsulated inside a given delivery system offers conditions which closely mimic the intended purpose of the carrier, i.e., the delivery of its cargo to a cell.

(40) Caruso, F. *Chem. Eur. J.* **2000**, *6*, 413−419.

(41) (a) Shi, X.; Caruso, F. *Langmuir* **2001**, *17*, 2036−2042. Caruso, F.; Yang, W.; Trau, D.; Renneberg, R. *Langmuir* **2000**, *16*, 8932−8936. Antipov, A. A.; Sukhorukov, G. B.; Donath, E.; Möhwald, H. *J. Phys. Chem. B* **2001**, *105*, 2281−2284. (b) Qiu, X.; Leporatti, S.; Donath, E.; Möhwald, H. *Langmuir* **2001**, *17*, 5375−5380. Qiu, X.; Donath, E.; Möhwald, H. *Macromol. Mater. Eng.* **2001**, *286*, 591−597. (c) Caruso, F.; Trau, D.; Möhwald, H.; Renneberg, R. *Langmuir* **2000**, *16*, 1485−1488.

(42) Claracq, J.; Santos, S. F. C. R.; Duhamel, J.; Dumousseaux, C.; Corpart J.-M. *Langmuir* **2002**, *18*, 3829−3835.

(43) Chiu, H.-C.; Chern, C.-S.; Lee, C.-K.; Chang, H.-F. *Polymer* **1998**, *39*, 1609−1616.

Second, the spectroscopic features of pyrene enable a detailed description of where pyrene is located and under which form it is while it is being unloaded from the delivery system. Third, all components used to demonstrate the efficacy of the carrier at delivering its hydrophobic cargo to a lipophilic environment (i.e., pyrene and the EPC lipid) are relatively cheap. All of these features contribute to making the procedure used in this report ideal to characterize how a given delivery system performs at unloading its hydrophobic cargo into a model cell membrane.

Over the past 10 years, sapeptides such as EAK have been under intense scrutiny.[2] It will be interesting to investigate whether the ability of EAK to stabilize a model hydrophobic compound in aqueous solution and deliver it into a cell mimic at a controlled rate can be extended to other peptide sequences.[44] Of particular interest are the studies of peptides designed to better adhere to[20] or translocate[21] cells with the aim of improving the uptake of the hydrophobic compound by the cell. Adhesion can be promoted by incorporating the Arg-Gly-Asp or Leu-Asp-Val sequences in a peptide,[20] whereas transportan[21a] and penetratin[21b] are examples of membrane translocating peptides. The peptide sequence can also be modified to optimize the subtle balance existing between hydrophilic and hydrophobic residues, which can be tuned to enhance the loading and release capacity of the peptide-based delivery system. The interactions of peptide made of all-D amino acids with microcrystals of hydrophobic compounds would be an interesting study as well, since such peptides have been shown to resist enzymatic degradation.[45] The ability of a peptide sequence to be tailored according to specific needs should make them desirable as effective biocompatible colloidal stabilizers of crystals of hydrophobic drugs.

Finally it must be noted that the large size of some of the EAK-PY aggregates might be detrimental to the use of EAK for the delivery of hydrophobic compounds into the bloodstream. As it turns out, particles smaller than 100 nm are required if they are to pass through fine capillaries.[46] For practical applications, particles with sizes of several microns such as those shown in Figure 9 must be made smaller in size. It must be noted however that the particle shown in Figure 9B appears to result from the aggregation of several smaller particles. In the future, it might be possible to modify the EAK coating by introducing some PEG functionality to stabilize the particles when their sizes is smaller than 1 μm and prevent their aggregation.

(44) Vauthey, S.; Santoso, S.; Gong, H.; Watson, N.; Zhang, S. *Proc. Nat. Aca. Sci.* **2002**, *99*, 5355−5360. Von Maltzahn, G.; Vauthey, S.; Santoso, S.; Zhang, S. *Langmuir* **2003**, *19*, 4332−4337.
(45) Wade, D.; Boman, A.; Wåhlin, B.; Drain, M.; Andreu, D.; Boman, H. S.; Merrifield, R. B. *Proc. Natl. Acad. Sci.* **1990**, *87*, 4761−4765.
(46) Kabanov, A. V.; Alakhov, V. Y. *Amphiphilic Block Copolymers: Self-Assembly and Applications*; Elsevier: The Netherlands, 1997.

Conclusion

We have demonstrated that the self-assembling EAK peptide can stabilize the microcrystals of a hydrophobic molecule in aqueous solution. Steady-state fluorescence spectra were acquired for the EAK05-PY solution mixed with EPC vesicles, a solution of pyrene in EPC vesicles, the EAK05-PY solution, and pyrene crystals. They show that pyrene is molecularly dissolved only when it is mixed with EPC vesicles. Time-resolved fluorescence excimer decays were carried out on these four samples and revealed that at equilibrium all the pyrene inside the microcrystals of the EAK05-PY solution was transferred to the vesicle membrane. These measurements also demonstrated that pyrene is present in the crystalline state when it is associated with EAK rather than being molecularly solubilized. Similar conclusions were reached when these experiments were duplicated using the EAK01-PY solution. Dynamic light scattering measurements ensured that the addition of EAK and/or pyrene did not affect the size of the EPC vesicles. The release behavior of pyrene from its EAK coating was studied by following the fluorescence of pyrene upon exposure to EPC vesicles as a function of time. Since the monomer signal was only due to that of pyrene molecules transferred to the vesicles, the concentration of pyrene transferred to the vesicles could be determined as a function of time by comparing the monomer signal to that of a calibration curve. This procedure yielded a series of profiles representing the pyrene concentration inside the vesicle versus time. The transfer rate constants were determined and found to be much slower when pyrene was released from the EAK05-PY solution than from the EAK01-PY solution. Scanning electron micrographs suggest that this effect is due to the nature of the interactions occurring between EAK and pyrene. The EAK01-PY solution exhibited elaborate lace-like structures which appear to enhance the release of pyrene. The pyrene crystals observed in the EAK05-PY solution displayed a thick peptide coating which inhibited the release of pyrene. Our results suggest that EAK may be a potential carrier for low molecular weight, water insoluble compounds whose release into lipid bilayers can be controlled by tuning the peptide-to-cargo molecular ratio.

Acknowledgment. This research was financially supported by the Natural Science and Engineering Research Council of Canada (NSERC). We would like to acknowledge helpful discussions with Sukhdeep Dhadwar and Yooseong Hong. J.D. is especially thankful to the financial help provided by a Premier Research Excellence Award and his being awarded a Tier-2 Canada Research Chair. P.C. thanks S. Zhang of MIT for many stimulating conversations. The help of Howard Siu who ran all the excimer fluorescence decays is dearly acknowledged.

JA0381297